Einstein's Electron and Local Branching: Unitarity without Many Worlds

Local Hilbert spaces, boundaries, and quantum nonlocality

Xing M. Wang[1]

Abstract

Traditional interpretations of quantum mechanics often present a dichotomy: either the wavefunction collapses upon measurement (Copenhagen), violating unitarity, or the entire universe branches into countless parallel worlds (Many-Worlds), with significant ontological proliferation. The Branched Hilbert Subspace Interpretation (BHSI) resolves this tension by introducing branching strictly within local Hilbert spaces. This framework reinterprets scenarios such as Einstein's 1927 electron-diffraction thought experiment, in which all quantum events are confined to a local Hilbert space, allowing the Born rule to emerge naturally from branch weights. Crucially, BHSI treats branching as a dynamical process tied to information recording. This leads to a testable proposal: a dual-layer experiment in which the particle transit time between layers is shorter than the sensor response time, enabling a direct probe of measurement timing and "mismatched" or "uncommitted" outcomes. We argue that a quantum system behaves as a unified whole—an "island of coherence"—within which unitary branching is confined to the system's boundary, without observable correlations with distant, unentangled systems. Finally, we show that quantum nonlocality (e.g., in Bell tests or tunneling) arises naturally from the intrinsic vector-space structure of local Hilbert spaces, rather than from superluminal signaling.

Keywords: Born Rule; Branched Hilbert Subspace Interpretation; Copenhagen Interpretation; Local Hilbert Space; Many-Worlds Interpretation; Quantum Nonlocality.

1. Introduction

In our previous article [1], we proposed the Branched Hilbert Subspace Interpretation (BHSI). In this framework, measurement is modeled as a sequence of unitary operators: branching, engaging, and disengaging within the local Hilbert space (LHS). The resulting branches are locally decoherent, evolve unitarily and independently, and the system's initial state determines their amplitudes—thereby encoding the Born rule. Notably, this branching is not necessarily terminal; branches may recohere before irreversibly entangling with the environment, as explored in detail in [2]. We have demonstrated that such locally controlled decoherent-recoherent processes are observable in protocols such as quantum teleportation ([3]; Sec. 5.2 of [1]). Building on this, we proposed experiments using modern Stern-Gerlach interferometers [4,5] to visualize the physical reality of branch weights, branch-dependent electromagnetic and gravitational phase shifts ([4,5], Sec. 5.3 of [1]), and probe the potential for recoherence [2].

[1] Sherman Visual Lab, Sunnyvale, CA 94085, USA; xmwang@shermanlab.com; ORCID:0000-0001-8673-925X

To directly probe local quantum branching, let us revisit Einstein's famous thought experiment presented at the 1927 Solvay Conference [6,7]. The experiment involved a screen with a small opening, through which electrons (or photons) were directed. Behind this screen was a large, hemispherical photographic film to record where the particles landed. Quantum theory describes particles as waves (de Broglie waves). These waves diffract at the opening, resulting in a distribution of particle detections on the film. According to the Copenhagen Interpretation (CI, [8, 9]), when an electron reaches a specific position on the film, it suddenly finds itself at that particular location, and the probability of finding it elsewhere vanishes simultaneously (a collapse). Einstein argues: "The interpretation, according to which [the square of the wave-function] expresses the probability that this particle is found at a given point, assumes an entirely *peculiar* mechanism of action at a distance, which prevents the wave continuously distributed in space from producing an action in two places on the screen." In 1927, Einstein called this action at a distance "peculiar," not "spooky, but they were referring to the same concept.

Einstein's thought experiment provides an ideal scenario for comparison between the Many-Worlds Interpretation (MWI, [10-12]), CI, and the BHSI. The setup of Einstein's thought experiment is now fully achievable with modern single-electron sources [13], sub-nanometer to few-nanometer scale pinhole [14,15], and nanosecond-resolution detector arrays. In the next section, we describe how to realize the experiment, ensuring that no signals propagate outside the closed system of the opaque hemisphere of modern opaque electron sensors [16,17]. In Section 3, we describe the process mathematically and compare the unitary branching of MWI with that of BHSI. In addition, we can record the uneven distribution pattern beforehand by employing a scintillating screen and an external optical camera [13, 18] to visualize the Born rule, encoded by the branch weights, as proposed by BHSI.

To further probe the dynamics of local branching, in Section 4, we propose a novel dual-layer detector system featuring a transparent inner hemisphere with transparent electron sensors [19, 20], aligned with the opaque sensors on the outer detector (dual sensing). The electron's transit time between layers is comparable to the reaction times of modern sensors. Crucially, this dual-layer design allows us to investigate scenarios of potential misaligned detections (e.g., inner #35 → outer #45), which would offer profound insights into the speed and completeness of quantum branching. In Section 5, we analyze all possible outcomes (normal or abnormal) of the dual-layer experiment, distinguishing interpretations side by side.

The observed absence of any wave amplitude beyond the opaque detector is naturally explained within the BHSI, in which the entire measurement process—including branching, engagement, and disengagement—occurs within the measured system. In Section 6, we formalize this viewpoint by exploring the concept of a *local Hilbert space* (LHS), defined as the bounded Hilbert space of a quantum system that behaves as a coherent, *inseparable whole* under measurement. Within such a space, quantum states are *intrinsically nonlocal*, since a Hilbert space is a vector space equipped with an inner product but no metric structure [21]. This intrinsic nonlocality gives rise to interference, tunneling, and Bell-type correlations without violating relativistic causality. Consequently, branching occurs only within the LHS of the measured system and doesn't extend to other systems that are not operationally entangled with it.

This leads to a powerful and parsimonious picture: each quantum system under observation is an "island of coherence," inseparable by observation, surrounded by a classical environment. Its correlations with other quantum "islands" are negligible unless they are deliberately entangled. Such islands may range from a pair of entangled photons to billions of Cooper pairs involved in macroscopic superconducting tunneling and, in principle, to astronomical objects such as white dwarfs and neutron stars [22-29].

This framework stands in clear contrast to the Many-Worlds Interpretation. Whereas MWI embeds all systems in a single, universally branching Hilbert space, BHSI confines physical branching to experimentally accessible domains defined by isolation and coherence. By clarifying the roles of boundaries and the intrinsic nonlocality of local Hilbert spaces, BHSI resolves the measurement problem in a way that preserves unitarity, aligns with laboratory practice and decoherence theory, and avoids the wavefunction collapse in CI, the ontological excess of MWI, and the explicit nonlocality of Bohmian mechanics [30-31].

2. Localizing Quantum Branching: Single-Layer Hemispheric Detector

The core experimental setup aims to realize a modern version of Einstein's thought experiment on electron diffraction, directly probing the quantum branching in a local Hilbert space.

A highly collimated beam of single electrons, each with an energy of approximately 1 keV, is emitted from a controlled source at a low rate, e.g., $f \sim 1$ MHz, ensuring 1 μs separation of individual electrons. This beam is directed through an exquisitely small pinhole, which induces significant diffraction of the electron's wave function. The diffracted electron then propagates towards a large, hemispherical detector array, positioned so that the pinhole effectively serves as the center of the sphere. This detector, with a radius $R \sim 10$ cm, comprises 1000 individually addressable opaque sensors (reaction time $\tau \sim 0.1$ ns), designed to register the arrival of a single electron (Fig. 1). The experiment focuses on recording the precise location (which sensor) and time of arrival for each electron.

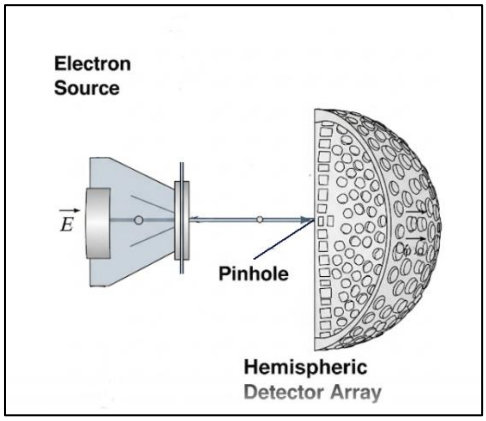

Fig. 1: Schematic Diagram of a Single-Layer Opaque Detector

The feasibility of constructing this primary experimental setup relies on remarkable advancements in modern electron and detector technologies, conducted under tightly controlled

environmental conditions. The entire experimental apparatus must operate under Ultra-High Vacuum (UHV) conditions, typically at a pressure below 10−9 Torr. This is essential to minimize electron scattering by residual gas molecules, which would otherwise obscure the delicate diffraction pattern. UHV also extends the cathode's lifespan and prevents contamination of the pinhole and detector surfaces. The experiment can generally be conducted at room temperature. However, precise temperature stabilization might be beneficial for long-term drift control, and some high-performance detectors may incorporate localized cooling to minimize noise.

Key components and their current technological status include:

- **Single-Electron Source:** Stable, high-brightness single-electron emission is routinely achieved with advanced Field Emission Guns (FEGs), commonly found in modern electron microscopes. These sources provide highly coherent electron beams suitable for single-electron experiments [13].
- **Pinhole:** The challenging sub-nanometer to few-nanometer scale pinhole required for significant electron diffraction is at the cutting edge of nanofabrication, but is achievable. Techniques such as Focused Ion Beam (FIB) milling or advanced Electron Beam Lithography (EBL) can sculpt apertures with nanometer precision [14, 15].
- **Hemispheric Detector Array:** The core of the detection system, this array can be realized by precisely tiling numerous high-performance direct electron detectors (DEDs), typically based on CMOS or Hybrid Pixel Array (HPA) technologies, onto a machined hemispheric support structure. These detectors offer single-electron sensitivity, rapid readout capabilities (with a reaction time of $\tau \sim 0.1$ ns and high frame rates), and high quantum efficiency with minimal dead space, making them ideal for single-electron counting experiments [16, 17].

3. Mathematical Description and Interpretations of the Procedure

The Initial State: When an electron is emitted through the pinhole, its wave propagates in the hemisphere. Because we only concern ourselves with the events in which the electron is detected by one of the $N = 1000$ sensors, the total wave function can be written in two parts:

$$|\Psi\rangle = a|\Psi_e\rangle + b|\Psi'\rangle, \quad |\Psi_e\rangle = \sum_{k=1}^{N} c_k |\psi_k\rangle, \quad \sum_{k=1}^{N} |c_k|^2 = 1, \quad \prod_{k=1}^{N} |c_k|^2 \neq 0, \quad N = 1000 \qquad (1)$$

Here, the wave part $|\Psi_e\rangle$ represents the initial state, a superposition of N possible outcomes with non-zero probabilities, as described by Eq. (1) of [1]; the wave part $|\Psi'\rangle$ represents any undetected electron events that occur when electrons are caught in the area between the sensors or on the bottom. The basis states of the initial state can be considered as the eigenstates of the operator of the sensor's serial number:

$$\hat{n}|\psi_k\rangle = k|\psi_k\rangle, \quad \langle\psi_i|\psi_k\rangle = \delta_{i,k}, \quad i,k \in \{1,2,\ldots,N\}, \quad N = 1000 \qquad (2)$$

3.1. BHSI Interpretation: The existence of $|\Psi\rangle$ means the quantum system is described by an inseparable wavefunction in a *single LHS.* The whole process can be described as follows.

The Branching: When the wave front touches the hemisphere (R ~ 10 cm), it starts the first operation of the measurement process, branching, as described by Eqs. (2-3) in [1]:

$$\hat{B}(|\Psi_e\rangle\otimes|E\rangle_L)\equiv|\Psi_B\rangle=\sum_{k=1}^{N}c_k\,|\psi_k\rangle\,|E_k\rangle_L=\sum_{k=1}^{N}c_k\,|\psi_{B;k}\rangle,\quad |\psi_{B;k}\rangle\equiv|\psi_k\rangle\,|E_k\rangle_L \tag{3}$$

The engaging-disengaging process: Assume sensor #35 registers a hit, we have the following engaging-disengaging process, $\Sigma_\beta \equiv \Gamma_\beta T_\beta \Lambda_\beta$, as outlined in Eqs. (4-6) in [1]:

$$|\Psi_B\rangle\otimes|\text{ready}\rangle_O\rightarrow\sum_{k=1}^{1000}c_k(1-\delta_{k,35})\,|\psi_{k,B}\rangle+c_{35}\,|\psi_{35,B}\rangle\,|\text{reads 35}\rangle_O\rightarrow|\Psi_B\rangle\otimes|\text{ready}\rangle_O \tag{4}$$

The relocating process: Because the electron is detected and absorbed by the sensor, there is *zero probability of finding the electron anywhere outside the hemisphere*. Therefore, the decoherent branches must have been entangled within the closed local environment:

$$U_E:|\Psi_B\rangle\otimes|E\rangle\rightarrow|E'\rangle \tag{5}$$

Otherwise, the conservation of energy, matter, and charge is violated.

3.2. Many-Worlds Interpretation (MWI):

According to MWI, when the electron interacts with the detector, the universe instantly branches into 1,000 decoherent worlds — one for each sensor that could have recorded the detection. Suppose sensor #35 in our world registers the electron. Then, in the 999 parallel but causally disconnected branches, the electron is detected by other sensors. The observer who reads "35" is simply the version of the original observer that became entangled with the sensor #35 outcome. Decoherence — the entanglement of the sensor with the global environment — prevents the branches from interfering with each other.

$$|\Psi_e\rangle\otimes|E\rangle_G\rightarrow\sum_{k=1}^{1000}c_k\,|\psi_k\rangle\,|E_k\rangle_G,\quad {}_G\langle E_j\,|\,E_k\rangle_G\rightarrow\delta_{j,k} \tag{6}$$

The rate of generating new worlds is about one billion per second in our lab setting. Notably, since each branch contains a complete and closed copy of the experimental system, the observed electron should leave no detectable signal beyond the hemispherical detector, preserving conservation of energy, matter, and charge in every branch.

3.3. Copenhagen Interpretation (CI):

In CI, when the electron interacts with sensor #35, the entire wavefunction — previously spread over all sensors — undergoes an instantaneous, non-unitary collapse to a single point. The probability of detecting the electron in the other 999 sensors instantly drops to zero. This collapse occurs at the moment of measurement, without a detailed account of its physical mechanism. Since the collapse reduces a spread-out wave into a sharply localized result instantaneously, it implies a form of nonlocality — the kind Einstein famously criticized as "spooky action at a distance."

3.4. Comparing Interpretations:

Both MWI and BHSI maintain unitary evolution and avoid the postulated collapse of CI.

However, they differ fundamentally in ontology. MWI asserts that all possible outcomes occur in parallel, real worlds, each branching irreversibly upon detection. In contrast, BHSI postulates a single, branching structure of local Hilbert subspaces within our world. Alternative branches exist temporarily but become inaccessible as they rapidly entangle with the environment. In this view, branching is real, but it occurs within a single universe and does not generate new, unobservable realities. The single-layer hemispherical experiment thus highlights the subtle but crucial difference between a local, single-world model (BHSI) and a global, many-worlds model (MWI), while preserving agreement on experimental predictions.

3.5. The Born Rule:

Moreover, the diffraction pattern need not be spherically symmetric; it can be shaped by adjusting the pinhole's size and geometry. In such cases, we can pre-record the expected intensity distribution optically by using a scintillating screen placed on the inner surface of a hemisphere (radius R about 10 cm, without sensors), paired with an external scientific camera (e.g., CMOS or CCD) [13,18]. This optical map, representing the probability density $|\Psi|^2$ according to the Born rule, provides a reference distribution against which we compare the detector click statistics. When the experiment is repeated with sensors on the opaque hemispheric detector, the observed click distribution, compiled over billions of emitted electrons, should match the pre-recorded intensity profile. In BHSI, this agreement arises naturally: the branch weights, defined by the squared amplitudes in each local Hilbert subspace, $|c_k|^2$, obey the Born rule and govern the statistical frequencies of detector outcomes.

4. Enhanced Experimental Setup: Dual-Layer Hemispheric Detector

To rigorously probe the subtle dynamics and completeness of the quantum measurement process, we propose an advanced dual-layer detector system (dual-sensing). This setup builds upon the single-layer experiment by introducing a second, inner hemispheric detector array that is critically transparent to the incoming electrons. The electron beam, after diffraction through the pinhole, first encounters the inner transparent detector, positioned at a radius of $R \sim 19.5$ cm. This layer comprises numerous (e.g., 200) individually addressable segments or sensors. After interacting with the inner layer, the electron continues its trajectory a very short distance, approximately 0.5 cm, to the 200 sensors at the outer opaque hemispheric detector ($R \sim 20$ cm), which is similar in design to the detector in the primary experiment. Both layers are precisely aligned, meaning each segment on the inner layer corresponds spatially to a specific segment on the outer layer. The experiment's core measurement involves recording "double-click" events: a correlated detection in both inner and outer layers within an extremely tight time window.

The extremely short physical separation of $\Delta R \sim 0.5$ cm between the detector layers, combined with the higher electron energy of 5 keV ($v \sim 4.2 \times 10^7$ m/s), yields a remarkably short electron transit time of $\Delta t \sim \Delta R/v \sim 0.12$ ns. This timescale is critical, as it is comparable to, or potentially even shorter than, the full 'reaction' or 'decision' time of the fastest modern transparent single-electron detectors ($\tau_{in} \sim 1$ ns).

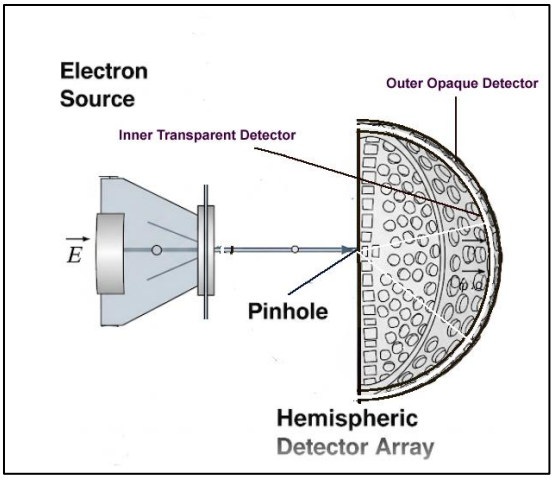

Fig. 2: Schematic Diagram of a Dual-Layer Hemispheric Detector

This unique temporal window enables the experiment to investigate whether the quantum measurement event initiated at the inner transparent detector is truly instantaneous and irreversible, or a dynamic process (a time-like sequence of space-time events) that takes a finite amount of time to complete. The electron source, operating at 5 keV, remains a standard Field Emission Gun (FEG) system capable of generating individual electrons in Ultra-High Vacuum (UHV) environments [13]. Similarly, the demanding nanometer-scale pinhole can be achieved through advanced FIB milling techniques [14]. The outer opaque hemispheric detector, composed of tiled direct electron detector (DED) modules (e.g., CMOS or hybrid pixel arrays), is also within current manufacturing capabilities, ensuring robust single-electron detection with high efficiency and precise timing (reaction time $\tau \sim 0.1$ ns).

The paramount technological challenge for this enhanced setup lies in the inner transparent hemispheric detector array. This component requires materials that are exceptionally thin yet robust (e.g., graphene, ultrathin silicon nitride, or amorphous carbon membranes) to minimize electron scattering and energy loss, ensuring that electrons propagate to the outer layer. Simultaneously, these transparent segments must be active detectors, capable of generating a measurable signal from a single 5 keV electron with a reaction time $\tau_{in} \sim 1$ ns, providing precise sub-nanosecond timing, and maintaining spatial addressability across hundreds of segments. Integrating active detection elements (such as highly sensitive 2D-material-based sensors or ultra-thin silicon structures) onto such large, curved, transparent substrates, while maintaining minimal interaction with passing electrons and providing rapid readout, represents the forefront of current detector research and fabrication science [19, 20]. While extremely ambitious, this component conceptually aligns with ongoing efforts in novel electron microscopy detectors and atomically thin material-based sensing, framing the dual-layer experiment as a powerful, aspirational grand challenge for foundational quantum physics.

The time window T_W (~6 ns) for counting any two successive clicks is set as follows:

$$\Delta t\,(\sim \Delta R / \mathrm{v} \sim 0.12\ \mathrm{ns}) \le \tau_{in}\,(\sim 1\mathrm{ns}) < T_W\,(\sim 6\,\mathrm{ns}) << 1/\ f\,(\sim 1\ \mu\mathrm{s}) \qquad (7)$$

Because the transit time Δt (~0.12 ns), plus the reaction time (τ ~0.1 ns) of the outer sensors, is approximately or shorter than the inner sensor reaction time (τ_{in} ~1 ns), we can expect possible "*delayed choices*" or "*uncommitted choice*" by the inner sensors during the test runs within the time window (T_W ~ 6 ns, which includes $\pm 3\sigma \sim \pm$ 3ns, the standard deviations).

We can also pre-record the wave distribution density on a scintillating screen placed on the inner surface of the outer hemisphere (radius $R \sim 20$ cm, without the inner detector layer) to visualize the branch weights, as already described in Section 3.4.

5. Interpretations of Possible Two-Layer Experimental Results

This two-layer detection setup allows us to probe when and how measurement-induced branching occurs by analyzing correlated detection events across three major categories.

5.1: **Aligned Detection**: Inner Sensor #35 → Outer Sensor #35.

This is the expected and dominant outcome: an electron passes through transparent sensor #35 in the inner layer. It is subsequently propagated to and absorbed by sensor #35, which is aligned in the outer layer. The two events are separated by a consistent time delay (within the ~6 ns window), confirming that they represent the same particle.

BHSI: Branching occurs locally at the inner sensor, where the electron's wavefunction decoheres into 200 branches. One branch engages/disengages with sensor #35 with the probability $|c_{35}|^2$, and propagates to the outer sensor, deterministic and unitary, as described by Case 1 in Section 2.2 of [1], for the basis state $|\psi_{35}\rangle$. All 200 branches, $|\psi_{k,B}\rangle$, are relocated to the environment before reaching the outer layer. This preserves a single-world ontology while explaining the Born rule naturally from the amplitudes of the initial state.

MWI: The electron evolves into a superposition of all possible paths, each corresponding to a different world. The observer experiences one outcome (e.g., #35 → #35), while the other 199 outcomes exist in parallel but inaccessible worlds. This is consistent with MWI but leaves the ontology bloated and unverifiable in practice.

CI: The wavefunction collapses instantaneously at the inner detector (#35), and the particle is then treated classically en route to the outer detector. However, the fact that all other inner sensor probabilities drop to zero instantaneously raises Einstein's concern about "spooky action at a distance."

5.2: Misaligned Detection: Inner Sensor #35 → Outer Sensor #45.

Rare but possible outcomes, where the inner sensor #35 fires, but the outer detection occurs at a different location (e.g., #45), within the timing window (~ 0.6 ns). They may reflect a slight scattering in the transparent layer or detector misalignment. Otherwise:

- **BHSI:** It may imply that the branch $|\psi_{45,B}\rangle$ arrives at the outer layer before the inner sensor #35 has registered (a "*delayed choice*"?). Since BHSI models measurement as a sequence of local, unitary events (branching, engaging, disengaging, relocalizing), such anomalies are fully compatible and potentially informative for estimating the actual timescale of the events.

- **MWI:** MWI assumes global, timeless branching. A mismatch in real-time detection challenges this view, especially if the inner sensor registers first. MWI lacks a mechanism to explain how a superposition “chooses” a mismatched outer outcome in a given branch without violating its principle of simultaneity.
- **CI:** This result directly contradicts the idea of instantaneous wavefunction collapse at the inner sensor. If the particle's position was fixed at #35, why would it appear at #45 later?

5.3: One Outer Detection Only. No inner sensing → Outer Sensor #45.

In this scenario, the outer opaque detector registers the electron, but the corresponding inner transparent sensor fails to record a signal. While often attributed to detector inefficiency, the consistent statistical occurrence of these events suggests a "Temporal Threshold Effect" unique to BHSI. Such an outcome is a natural prediction of BHSI, in which measurement is a local, time-extended process that culminates in disengagement or environmental entanglement. It would, however, challenge interpretations that posit an instantaneous, discontinuous change at the first possible moment of interaction (the "Heisenberg cut" in Copenhagen, or the global branching implied by MWI at the decoherence time). This scenario directly probes the *temporal structure of measurement*, a question BHSI is explicitly designed to address

The diagnostic power of this dual-layer setup lies in its ability to create a clean empirical testbed. It allows us to distinguish between interpretations by directly probing the time-resolved and local nature of quantum measurement. Even if most outcomes are consistent across multiple interpretations, subtle anomalies (Sections 5.2 or 5.3) could provide discriminating empirical evidence in favor of a local Hilbert space in single-world ontology as proposed by BHSI.

Note: Scenarios involving apparent violations of energy or particle conservation (e.g., duplicate detections on inner or outer layer only) are excluded from consideration, as such events would indicate experimental artifacts or a breakdown of quantum theory itself rather than differences between interpretations.

6. Boundary and Nonlocality of Local Hilbert Spaces

Throughout this paper, we emphasize that quantum measurements occur within local Hilbert spaces. It is therefore essential to clarify what is meant by a “local Hilbert space,” why such spaces exist, and how their intrinsic properties allow for unitary branching without necessitating a global "Many-Worlds" split.

6.1: Definition and the "Island" Ontology

A local Hilbert space (LHS) is the mathematical domain associated with a quantum system—microscopic, mesoscopic, or macroscopic—that is *operationally* isolated from its environment. This isolation is defined by a *quantum boundary*: a threshold at which the correlation (decoherence) between the system (Q_0) and its environment (E) is sufficiently low—as defined by the relevant measurement context—to permit the system's coherent unitary evolution.

This boundary separates the system from surrounding classical or quantum systems, effectively defining a local tensor-product factorization of the total state space, in which Q_0 does not form an inseparable quantum whole with E, as in Eq. (8) below.

The system may range in scale from a pair of entangled photons to macroscopic coherent objects like superconductors or even neutron stars. What defines the system is not its spatial extent, but its *inseparability*: the fact that its quantum state behaves as a unified entity. Within the experimental context, the system cannot be further subdivided into independently measurable subsystems without destroying the measurement's coherence.

Conceptually, a local Hilbert space may be viewed as an "island" of quantum coherence embedded in a predominantly classical environment. Although a hypothetical universal ("World") wavefunction $|\mathrm{W}\rangle$ may be formally defined in principle, BHSI treats it as physically inoperative. Observable physics is instead described in terms of separable classical (C) systems and inseparable quantum (Q) systems, each associated with its own operational domain. When Q_0 is measured, the dynamics are strictly confined to Q_0's local Hilbert space, effectively partitioning the World state and its probability density into functionally independent domains:

$$\begin{aligned} &|\mathrm{W}\rangle \to \bigotimes_i |C_i\rangle \bigotimes_\mu |Q_\mu\rangle \to |Q_0\rangle; \\ &\rho(\mathrm{W}) \to \bigotimes_i \rho(C_i) \bigotimes_\mu \rho(Q_\mu) \to \mathrm{Tr}_E \rho(\mathrm{W}) \to \rho(Q_0), \quad \text{where } Q_0 \notin E \end{aligned} \tag{8}$$

Here, the indices i label classical subsystems, μ label quantum subsystems, and E denotes all degrees of freedom external to the local Hilbert space of Q_0. The final expressions represent the effective quantum state relevant for measurement, obtained by tracing over inaccessible environmental degrees of freedom and renormalization.

The existence of local Hilbert spaces is not a fundamental metaphysical postulate but a consequence of *the conditions required for quantum measurement*: any quantum experiment requires isolating the system of interest from uncontrolled environmental degrees of freedom to a sufficient degree. The boundaries of these "islands" are not arbitrary; they are dynamically maintained by environmental decoherence, which acts as the dissipative "current" of the classical ocean, suppressing interference between the system and its surroundings. Unlike the Many-Worlds Interpretation, which splits the entire ocean with every measurement, BHSI posits that branching is a localized event, strictly confined to the island's boundary.

6.2: The Intrinsic Nonlocality of a Local Hilbert Space (LHS)

A Hilbert space (or its rigged extension for continuous spectra [21]) is fundamentally a vector space equipped with an inner product. Crucially, it lacks a metric corresponding to spatial distance. Quantum states are vectors characterized by direction and magnitude within this vector space. This has a direct and profound consequence for spatial description. In the coordinate representation, distinct spatial positions $\boldsymbol{x}$ and $\boldsymbol{x}'$ ($\boldsymbol{x} \neq \boldsymbol{x}'$) correspond to two orthogonal basis vectors $|\boldsymbol{x}\rangle$ and $|\boldsymbol{x}'\rangle$, regardless of their physical distance $|\boldsymbol{x} - \boldsymbol{x}'|$:

$$\text{Hilbert Space: } \langle \boldsymbol{x} | \boldsymbol{x}' \rangle = 0 \text{ for } \boldsymbol{x} \neq \boldsymbol{x}' \Leftrightarrow \text{Metric Space: } |\boldsymbol{x} - \boldsymbol{x}'| > 0 \text{ for } \boldsymbol{x} \neq \boldsymbol{x}' \tag{9}$$

Likewise, the wave function amplitudes $\langle x|\Psi\rangle = \Psi(x)$ and $\langle x'|\Psi\rangle = \Psi(x')$ are not separated by any notion of distance in the Hilbert space; they are different components of the same state vector expressed in a chosen basis.

Consequently, a quantum system described within a single Local Hilbert Space (LHS) behaves as an inseparable whole with respect to its Hilbert-space properties. This intrinsic, non-spatial nonlocality is the foundational mechanism behind quantum tunneling, interference, and—critically—the nonlocal correlations observed in entangled systems [22-29]. These phenomena do not imply superluminal signaling or violate relativistic causality, because "influence" within a Hilbert space is not a causal process propagating through spacetime; it is a mathematical expression of the state's coherence.

Two quantum systems are described by distinct local Hilbert spaces if they can be prepared, manipulated, and measured independently—that is, if they do not form a coherent, entangled whole. Conversely, if two systems are prepared in an entangled state and their coherence is preserved, they constitute a single composite quantum system, described by a single LHS, irrespective of their spatial separation. This is precisely the case in a Bell-type experiment [22, p. 25]. A source generates a pair of photons in an entangled polarization state, such as one of the Bell states:

$$|\Phi^{\pm}\rangle = \frac{1}{\sqrt{2}}(|H\rangle_A|H\rangle_B \pm |V\rangle_A|V\rangle_B),\ |\Psi^{\pm}\rangle = \frac{1}{\sqrt{2}}(|H\rangle_A|V\rangle_B \pm |V\rangle_A|H\rangle_B) \tag{10}$$

This state does not reside in two separate 2D Hilbert spaces for photons *A* and *B*; it is a non-separable vector in the 4D tensor-product space $H_A \otimes H_B$, which forms the LHS for this composite system. If the photons are spatially separated while maintaining entanglement (i.e., without decohering into a separable mixture), they continue to occupy this single, non-spatially-local LHS. Its "boundary" encloses the coherent connection, not the spatial volume.

Consequently, measurements on *A* and *B* are not independent operations on two systems; they are operations within the same composite system. In BHSI, branching relative to the measured observable (e.g., polarization) occurs locally within this composite LHS. This explains the observed nonlocal correlations as a consequence of the *intrinsic nonlocality* of the shared LHS, not as "spooky action-at-a-distance" through spacetime (rejected by Bell), nor as a manifestation of a universally branching wavefunction (MWI), nor as guidance by a nonlocal pilot-wave function (Bohmian mechanics [30-31]).

6.3: Mathematical Linking: Local Operators and Subspace Dynamics

The existence of the initial state vector $|\Psi\rangle$ associates the electron-diffraction system with a bounded local Hilbert space $\mathcal{H}_L$, providing the necessary "theater" for the BHSI operational sequence. In this interpretation, the transition from a quantum superposition to a definite classical record is not a global event but a sequence of unitary transformations of the state vector $|\Psi\rangle$ strictly within $\mathcal{H}_L$.

6.3.1. Branching (*B*): Within the "island" $\mathcal{H}_L$, the branching operator ***B*** partitions the local state into decoherent subspaces (see Eq. (3) above and Eq. (3) of [1]):

$$\begin{aligned}&\hat{B}:|\Psi\rangle\rightarrow|\Psi_B\rangle=\sum_{k=1}^{D}c_k\,|g_k\rangle\,|E_k\rangle_L\equiv\sum_{k=1}^{D}c_k\,|g_{B;k}\rangle,\quad {}_L\langle E_j\,|\,E_k\rangle_L\approx\delta_{j,k}\\&\hat{B}\left(\mathcal{H}_S\otimes\mathcal{H}_{L,E}\right)=\bigoplus_{k=1}^{D}\mathcal{H}_{S,k}(\text{span c}_k\,|\,g_{B;k}\rangle),\quad |\langle g_k\,|\,\Psi\rangle|^2=|\langle g_{B;k}\,|\,\Psi_B\rangle|^2=|\,c_k\,|^2\end{aligned}\tag{11}$$

Because the LHS is operationally isolated, branching ***B*** acts *only* within $\mathcal{H}_L$. The resulting state $|\Psi_B\rangle$ remains a single, inseparable vector in $\mathcal{H}_L$, but its components are now dynamically independent. Unlike MWI, there is no global action on a universal wave function, nor is a preferred frame of reference required to define the branches.

6.3.2. Engaging (Λ_β) and Disengaging (Γ_β): The observer's interaction with the branched system is represented by a local engagement operator Λ_β that correlates the observer's state with a specific branch $|g_\beta\rangle$ in accordance with the Born weights $|c_\beta|^2$ (see Eq. (4-5), [1]):

$$\Lambda_\beta:|\,\text{ready}\rangle_o\in\mathcal{H}_E\mapsto|\,\text{reads}\,g_\beta\,\rangle_o\in\mathcal{H}_{S,\beta},\quad \beta\in\{1.2.\cdots D\}\tag{12}$$

Because $\mathcal{H}_L$ is local, this engagement does not "drag" the rest of the universe into a split. After recording the outcome, operator T_β changes the observer's state to |ready⟩, then operator Γ_β disengages him from the branch. This operator effectively "seals" the boundary of the local Hilbert space, thereby effectively completing the measurement cycle. The branches are eventually unitarily relocated into the environment, becoming effectively suppressed through decoherence while maintaining unitary integrity (see Eq. (7, 24), [1]):

$$T_\beta:|\,\text{reads}\rangle_O\mapsto|\,\text{ready}\rangle_O;\quad \Gamma_\beta T_\beta:\mathcal{H}_B\mapsto\mathcal{H}_f=\left\{\bigoplus_{k=1}^{D}\mathcal{H}_{S,k}(\text{span}\,c_k\,|\,g_{B,k}\rangle\right\}\otimes|\,\text{ready}\rangle_O\tag{13}$$

$$U_E:|\,\Psi_B\rangle\otimes|\,E\,\rangle\rightarrow|\,E'\,\rangle\tag{14}$$

In BHSI, these unitary operators serve as a functional alternative to "collapse." They provide a definitive outcome for the local observer without violating the relativity of simultaneity for distant systems. This marks the fundamental distinction from MWI: while MWI subsumes all systems into a single universal Hilbert space—triggering global branching—BHSI confines the physical realization of outcomes to the empirically accessible domain of the local Hilbert space.

6.4: Examples of Local Hilbert Spaces for Various Quantum Systems

The Local Hilbert Space (LHS) is not a mathematical abstraction but a description of the domain of coherence for any physical system exhibiting quantum behavior. Its defining feature is the existence of a boundary—enforced by experimental isolation or intrinsic dynamics—within which the system must be treated as an inseparable quantum whole, as defined in Section 6.1.

The electro-diffraction experiments analyzed in this paper are prime examples of such a system. This principle applies universally:

Microscopic/Mesoscopic: Entangled photon pairs in Bell-type experiments [22], single atoms undergoing quantum tunneling [23], and hybrid systems such as a photon entangled with a trapped ion in a high-finesse cavity [24] are all well-described by local Hilbert spaces defined by experimentally maintained coherence and isolation.

Macroscopic: Superconductors and superfluids, such as the billions of electron Cooper pairs in macroscopic superconducting tunneling [25], where a single wave function describes a collective state. Notably, parallel quantum computing is more parsimoniously described as the evolution of parallel local Hilbert subspaces rather than the splitting of the device into parallel worlds [25].

Astrophysical: On much larger scales, compact astrophysical objects such as white dwarfs [26] and neutron stars [27] can be modeled, to good approximation, as quantum systems in which degeneracy pressure—a purely quantum effect—governs the macroscopic equilibrium of the entire object. Even black holes have been proposed to admit an effective description as condensates of soft gravitons in certain approaches to quantum gravity [28].

In every case, the LHS is the physically operative domain for quantum dynamics. This framework is consistent with all empirical evidence: quantum correlations are observed only between systems that share a coherent link (i.e., are part of the same LHS). Crucially, no experiment has ever shown that a measurement on one isolated quantum system (one LHS) induces a physical change or branching in a distant system (a separate LHS), whether in an adjacent lab or across astronomical distances. BHSI provides the natural language for this fundamental observational constraint.

7. Summary and Discussion

Three central features characterize the Branched Hilbert Subspace Interpretation (BHSI). First, a quantum system under measurement is described as an "island of coherence": a local Hilbert space (LHS) that is intrinsically nonlocal and inseparable under observation because of its metric-free vector-space structure. Second, quantum measurement is treated as a time-extended dynamical process of unitary operations, whose internal structure may become experimentally accessible as detection technologies advance. Third, local branching remains potentially reversible via recoherence before the system permanently entangles with the environment.

To explore the ontological and dynamical implications of this framework, we have revisited and modernized Einstein's 1927 diffraction thought experiment [6,7]. In the single-layer setup, an electron diffracts through a pinhole and is absorbed by a hemispherical array of position-resolved detectors. This arrangement shows that unitary branching can be confined entirely to a local Hilbert space and does not require global wavefunction splitting. Within BHSI, local branching preserves unitarity and the Born rule without invoking wavefunction collapse, many-worlds interpretations, or ambiguities about the physical status of branches.

The proposed two-layer detector extends this analysis by incorporating a transparent inner detection layer with sensors aligned with those of the outer absorbing array. This configuration is designed to probe the timing and localization of branching during the measurement process. A key prediction of BHSI [1] is that branching is a local, time-extended dynamical process. Correlated inner–outer detection (dual sensing) events would be a direct signature of this picture. At the same time, deviations (mismatching or uncommitting) from perfect correlation could reveal the fine-grained sequence of branching, engagement, and disengagement. Note that dual sensing is also used in the proposed Stern-Gerlach experiments [2], where conditional recoherence may be observed. Alternative interpretations, such as the Copenhagen interpretations [8,9] or the Many-Worlds Interpretation [10-12], may require additional assumptions to account for such dynamical details, which BHSI naturally accommodates through its structured event sequence.

Together, these features support a coherent, layered view of physical reality. From BHSI's perspective, the world admits a description with two domains: in the macroscopic domain, matter and energy coexist with spacetime, whereas in the quantum domain, systems—whether microscopic or astronomical—coexist with local Hilbert spaces, which serve as "islands of coherence" embedded in a predominantly classical environment, and in which unitary dynamics and quantum correlations are physically realized.

In summary, BHSI offers a coherent perspective in the long-standing debate over quantum interpretation. It is more ontologically parsimonious than the Many-Worlds Interpretation, more dynamically explicit than the Copenhagen Interpretation, and avoids the explicit nonlocal dynamics of Bohmian mechanics. By taking unitary quantum mechanics seriously while restricting its physical application to empirically justified domains, BHSI provides a conservative yet conceptually clear account of quantum measurement. As experimental techniques continue to improve, it may become possible to address Einstein's nearly century-old concerns not solely through philosophical analysis, but also through controlled, potentially falsifiable quantum experiments.

Abbreviations

BHSI	Branched Hilbert Subspace Interpretation
CI	Copenhagen Interpretation
LHS	Local Hilbert Space
MWI	Many-Worlds Interpretation

References

1. Wang, X. M. Quantum measurement without collapse or many worlds: The Branched Hilbert Subspace Interpretation. *arXiv:2504.14791* (2025). https://doi.org/10.48550/arXiv.2504.14791

2. Wang, X. M. Probing local branching dynamics with Stern–Gerlach interferometers and dual sensing. *arXiv:2508.16019* (2025). https://doi.org/10.48550/arXiv.2508.16019

3. Ursin, R., Jennewein, T., Aspelmeyer, M., et al. Quantum teleportation across the Danube. *Nature* 430, 849–849 (2004). https://doi.org/10.1038/430849a

4. Margalit, Y., Dobkowski, O., Zhou, Z., et al. Realization of a complete Stern–Gerlach interferometer: Towards a test of quantum gravity. *Sci. Adv.* 7, eabg2879 (2021). https://doi.org/10.1126/sciadv.abg2879

5. Bose, S., Mazumdar, A., Morley, G. W., et al. A spin entanglement witness for quantum gravity. *Phys. Rev. Lett.* 119, 240401 (2017). https://doi.org/10.1103/PhysRevLett.119.240401

6. Bohr, N. General discussion at the Fifth Solvay Conference (1927). In: *Niels Bohr Collected Works*, Vol. 6, pp. 99–106 (Elsevier, 1985).

7. Hossenfelder, S. What did Einstein mean by "spooky action at a distance"? Public lecture transcript (2021).

8. Bohr, N. Can quantum-mechanical description of physical reality be considered complete? *Phys. Rev.* 48, 696–702 (1935). https://doi.org/10.1103/PhysRev.48.696

9. Dirac, P. A. M. *The Principles of Quantum Mechanics*, 2nd ed. (Oxford University Press, 1935).

10. Everett, H. "Relative state" formulation of quantum mechanics. *Rev. Mod. Phys.* 29, 454–462 (1957).

11. Wallace, D. *The Emergent Multiverse* (Oxford University Press, 2012).

12. Vaidman, L. Why the many-worlds interpretation? *Quantum Rep.* 4, 264–271 (2022). https://doi.org/10.3390/quantum4030019

13. Egerton, R. F. *Physical Principles of Electron Microscopy* (Springer, 2005).

14. Gadgil, V. J., Tong, H. D., Cesa, Y., Bennink, M. L. Fabrication of nanostructures in thin membranes with focused ion beam technology. *Surf. Coat. Technol.* 203, 2436–2441 (2009). https://doi.org/10.1016/j.surfcoat.2009.02.036

15. Shahali, H., Hasan, J., Wang, H., et al. Evaluation of particle beam lithography for fabrication of metallic nanostructures. *Procedia Manuf.* 30, 261–267 (2019). https://doi.org/10.1016/j.promfg.2019.02.038

16. Faruqi, A. R., McMullan, G., et al. Electron detectors for electron microscopy. *Microsc. Today* 24, 34–41 (2016). https://doi.org/10.1017/S0033583511000035

17. Mendez, J. H., Mehrani, A., Randolph, P., Stagg, S. Throughput and resolution with a next-generation direct electron detector. *IUCrJ* 6, 1007–1013 (2019). https://doi.org/10.1107/S2052252519012661

18. Holst, G. C., Lomheim, T. S. *CMOS/CCD Sensors and Camera Systems*, 2nd ed. (JCD Publishing, 2011).

19. Hassan, J. Z., Raza, A., Babar, Z. U. D., et al. 2D material-based sensing devices: An update. *J. Mater. Chem. A* 11, 1–23 (2023). https://doi.org/10.1039/D2TA07653E

20. Ratti, L., Brogi, P., Collazuol, G., et al. Layered CMOS SPADs for low-noise detection of charged particles. *Front. Phys.* 8, 607319 (2020). https://doi.org/10.3389/fphy.2020.607319

21. Madrid, R. The role of the rigged Hilbert space in quantum mechanics. *Eur. J. Phys.* 26, 287–312 (2005). https://doi.org/10.1088/0143-0807/26/2/008

22. Nielsen, M. A., Chuang, I. L. *Quantum Computation and Quantum Information*, 10th Anniversary ed. (Cambridge University Press, 2010).

23. Hartman, T. E. Tunneling of a wave packet. *J. Appl. Phys.* 33, 3427–3433 (1962). https://doi.org/10.1063/1.1702424

24. Köbel, P., Breyer, M., Köhl, M. Deterministic spin–photon entanglement from a trapped ion in a fiber Fabry–Perot cavity. *npj Quantum Inf.* 7, 6 (2021). https://doi.org/10.1038/s41534-020-00338-2

25. Martinis, J. M., Devoret, M. H., Clarke, J. Energy-level quantization in the zero-voltage state of a current-biased Josephson junction. *Phys. Rev. Lett.* 55, 1543–1546 (1985). https://doi.org/10.1103/PhysRevLett.55.1543

26. Cuffaro, M. Many worlds, the cluster-state quantum computer, and the problem of the preferred basis. *Stud. Hist. Philos. Mod. Phys.* 43, 35–42 (2012). https://doi.org/10.1016/j.shpsb.2011.11.007

27. Chandra, V., et al. Observation of long-theorized quantum phenomena in astrophysical systems. *Astrophys. J.* 899, 146 (2020). https://doi.org/10.3847/1538-4357/aba8a2

28. Baym, G., Pethick, C., Pines, D. Superfluidity in neutron stars. *Nature* 224, 673–674 (1969). https://doi.org/10.1038/224673a0

29. Ciliberto, G., Balbinot, R., Fabbri, A., Pavloff, N. Quantum backreaction in an analog black hole. *Phys. Rev. A* 112, 063323 (2025).

30. Bohm, D. A suggested interpretation of the quantum theory in terms of "hidden" variables. I & II. *Phys. Rev.* 85, 166–193 (1952).

31. de Broglie, L. *On the Theory of Quanta*. PhD Thesis, University of Paris (1924).